Myocardin is required for maintenance of vascular and visceral smooth muscle homeostasis during postnatal development

Jianhe Huang[a], Tao Wang[a], Alexander C. Wright[b], Jifu Yang[a], Su Zhou[a], Li Li[a], Jisheng Yang[a], Aeron Small[a], and Michael S. Parmacek[a,c,1]

[a]Cardiovascular Institute and Departments of [b]Radiology and [c]Medicine, University of Pennsylvania Perelman School of Medicine, Philadelphia, PA 19104

Edited by Harry C. Dietz, Johns Hopkins University School of Medicine, Baltimore, MD, and approved February 27, 2015 (received for review October 23, 2014)

Myocardin is a muscle-restricted transcriptional coactivator that activates a serum response factor (SRF)-dependent gene program required for cardiogenesis and embryonic survival. To identify myocardin-dependent functions in smooth muscle cells (SMCs) during postnatal development, mice harboring a SMC-restricted conditional, inducible *Myocd* null mutation were generated and characterized. Tamoxifen-treated *SMMHC-Cre^{ERT2}/Myocd$^{F/F}$* conditional mutant mice die within 6 mo of *Myocd* gene deletion, exhibiting profound derangements in the structure of great arteries as well as the gastrointestinal and genitourinary tracts. Conditional mutant mice develop arterial aneurysms, dissection, and rupture, recapitulating pathology observed in heritable forms of thoracic aortic aneurysm and dissection (TAAD). SMCs populating arteries of *Myocd* conditional mutant mice modulate their phenotype by down-regulation of SMC contractile genes and up-regulation of extracellular matrix proteins. Surprisingly, this is accompanied by SMC autonomous activation of endoplasmic reticulum (ER) stress and autophagy, which over time progress to programmed cell death. Consistent with these observations, *Myocd* conditional mutant mice develop remarkable dilation of the stomach, small intestine, bladder, and ureters attributable to the loss of visceral SMCs disrupting the muscularis mucosa. Taken together, these data demonstrate that during postnatal development, myocardin plays a unique, and important, role required for maintenance and homeostasis of the vasculature, gastrointestinal, and genitourinary tracts. The loss of myocardin in SMCs triggers ER stress and autophagy, which transitions to apoptosis, revealing evolutionary conservation of myocardin function in SMCs and cardiomyocytes.

smooth muscle cell | transcriptional coactivator | autophagy | ER stress | apoptosis

The unique physiology and contractile properties of smooth muscle cells (SMCs) underlie their capacity to regulate arterial tone as well as gastrointestinal and genitourinary function. In contrast to striated muscle cells, SMCs maintain the capacity to proliferate and modulate their phenotype from a contractile to a synthetic state during postnatal development (for review, see ref. 1). The myocardin family of transcriptional coactivators (MRTFs), which includes myocardin, MKL-1/MRTF-A, and MKL-2/MRTF-B, are coexpressed in cardiomyocytes and SMCs, where they transduce signals from RhoA through the actin cytoskeleton, activating a subset of SRF-dependent genes encoding contractile and cytoskeletal elements (for review, see refs. 2–4). Mice harboring a null mutation in the myocardin gene (*Myocd*) exhibit a block in cardiomyocyte proliferation accompanied by a dramatic increase in cardiomyocyte apoptosis, leading to lethality at midgestation (5). Ablation of *Myocd* in the adult heart leads to heart failure and lethality attributable to a disruption in sarcomere structure accompanied by programmed cell death (6). By contrast, mice harboring a neural crest-restricted ablation of *Myocd* die in the perinatal period from patent ductus arteriosus (PDA) attributable to a block in the SMC contractile gene program (7).

After more than a decade of study, fundamental questions regarding the function of myocardin in vascular SMCs during postnatal development as well as visceral SMCs populating the gastrointestinal and genitourinary tracts remain unanswered. Is myocardin required for SMC contractile gene expression and maintenance of arterial tone? What role, if any, does myocardin play in regulating expression of SRF-regulated SMC contractile genes in visceral SMCs? Do the related transcriptional coactivators MKL-1 and/or MKL-2 mediate redundant functions with myocardin in the adult vasculature or visceral tissues (4)? Is myocardin required for survival of vascular SMCs in a manner analogous to that it plays in cardiomyocytes (7)? Is the loss of myocardin associated with predisposition to vascular proliferative syndromes including atherosclerosis and/or aortic aneurysm and dissection? In this regard, it is noteworthy that mutation in the SRF-activated genes *ACTA2*, *MYH11*, and *MYLK* are associated with heritable forms of TAAD (for review, see ref. 8).

In this report, we generated and characterized mice in which the *Myocd* gene was conditionally ablated in SMCs populating the adult vasculature and visceral tissues. Ablation of *Myocd* leads to profound defects in the structure of arteries as well as the gastrointestinal and genitourinary tracts. In the vasculature, this is accompanied by cell autonomous loss of the contractile

Significance

Smooth muscle cells (SMCs) play critical roles in maintaining organismal homeostasis. Myocardin is a muscle-restricted transcriptional coactivator previously implicated in development of the heart and vasculature. To define myocardin-mediated functions during postnatal development, we generated mice harboring an inducible, SMC-restricted mutation in the *Myocd* gene. Myocardin mutant mice exhibit profound derangements in arterial structure and in the gastrointestinal and genitourinary tracts. *Myocd* deletion leads to the loss of the contractile SMC phenotype, triggering cell-autonomous ER stress, autophagy, and apoptosis. These data reveal that myocardin is required for maintenance, homeostasis, and ultimately survival of vascular and visceral SMCs during postnatal development. These findings provide unanticipated insights into the pathogenesis of thoracic aortic aneurysm and dissection and gastrointestinal and genitourinary syndromes.

Author contributions: J.H., T.W., A.C.W., and M.S.P. designed research; J.H., T.W., A.C.W., Jifu Yang, S.Z., L.L., Jisheng Yang, and A.S. performed research; J.H. and M.S.P. contributed new reagents/analytic tools; J.H., T.W., Jifu Yang, S.Z., L.L., Jisheng Yang, A.S., and M.S.P. analyzed data; and J.H. and M.S.P. wrote the paper.

The authors declare no conflict of interest.

This article is a PNAS Direct Submission.

Freely available online through the PNAS open access option.

[1]To whom correspondence should be addressed. Email: michael.parmacek@uphs.upenn.edu.

This article contains supporting information online at www.pnas.org/lookup/suppl/doi:10.1073/pnas.1420363112/-/DCSupplemental.

gene program that occurs coincident with activation of endoplasmic reticulum (ER) stress and the autophagic program. However, over time, myocardin-deficient vascular SMCs undergo programmed cell death. These data provide conclusive evidence that myocardin is required for homeostasis of the vasculature and visceral tissues during postnatal development. Moreover, these data demonstrate that loss of myocardin in the postnatal vasculature triggers autophagy, which transitions to apoptosis and cell death.

Results

Generation of Mice Harboring an Inducible SMC-Restricted Null Mutation in the *Myocd* Gene. To elucidate functions mediated by myocardin in vascular and visceral SMCs during postnatal development, *SMMHC-Cre^{ERT2}/Myocd$^{F/F}$* conditional mutant mice were generated harboring a tamoxifen-inducible, SMC-restricted null mutation in the *Myocd* gene (Fig. S1*A*). Deletion of exon 8 generates a functionally null *Myocd* gene encoding a protein that cannot bind SRF or activate SRF-dependent genes (7). Quantitative RT-PCR (qRT-PCR) revealed an 85% decrease in myocardin mRNA in the aorta of tamoxifen-treated *SMMHC-Cre^{ERT2}/Myocd$^{F/F}$* mutant versus *Myocd$^{F/F}$* control mice (Fig. S1 *B* and *C*). By contrast, comparable levels of myocardin mRNA was observed in the hearts of tamoxifen-treated *SMMHC-Cre^{ERT2}/Myocd$^{F/F}$* mutants and control mice. Consistent with these findings, marked attenuation of nuclear myocardin protein was observed in the aorta of tamoxifen-treated *SMMHC-Cre^{ERT2}/Myocd$^{F/F}$* compared with *Myocd$^{F/F}$* control mice (Fig. S1 *D–F* and *I*). Interestingly, 14 d following tamoxifen treatment, a dramatic induction in cytoplasmic Mkl-1 (Fig. S1 *G* and *J*) and nuclear Mkl-2 (Fig. S1 *H* and *K*) was observed in aortic SMCs. These data demonstrate that *SMMHC-Cre^{ERT2}/Myocd$^{F/F}$* conditional mutant mice represent a strong hypomorphic phenotype attributable to near complete ablation of the *Myocd* gene in SMCs and that *Myocd* gene ablation induces expression of Mkl-1 and Mkl-2 in vascular SMCs.

SMC Conditional *Myocd* Ablation in Adult Mice Leads to Lethality. To define functions mediated by myocardin in SMCs during postnatal development, 6-wk-old *SMMHC-Cre^{ERT2}/Myocd$^{F/F}$* conditional mutant ($n = 60$) and *Myocd$^{F/F}$* control ($n = 60$) mice were treated with tamoxifen. After 14 d, no obvious differences in activity were observed between *SMMHC-Cre^{ERT2}/Myocd$^{F/F}$* conditional mutant and *Myocd$^{F/F}$* control mice. However, although no significant difference in body weight was observed between *SMMHC-Cre^{ERT2}/Myocd$^{F/F}$* ($n = 8$) and *Myocd$^{F/F}$* ($n = 8$) mice before tamoxifen exposure (18.9 ± 0.7 g versus 18.8 ± 0.6 g, P = nonsignificant), after 4 mo the mean body weight of *Myocd$^{F/F}$* controls was 30.8 ± 0.7 g versus 22.8 ± 0.7 g in *SMMHC-Cre^{ERT2}/Myocd$^{F/F}$* conditional mutants ($P < 0.001$). Moreover, 4 wk following treatment, ∼6% of *SMMHC-Cre^{ERT2}/Myocd$^{F/F}$* mice had died (Fig. 1*A*). Six months following *Myocd* ablation, ∼80% of *SMMHC-Cre^{ERT2}/Myocd$^{F/F}$* mice had died and no conditional mutant mice survived beyond 10 mo (Fig. 1*A*). By contrast, no deaths were observed in tamoxifen-treated *Myocd$^{F/F}$* control mice over 10 mo ($n = 60$) (Fig. 1*A*). These data demonstrate that SMC expression of myocardin is required for survival of adult mice and expression of the closely related *Mkl-1* and *Mkl-2* genes cannot compensate for the loss of myocardin in SMCs during postnatal development.

Loss of Myocardin Is Accompanied by Deformation of Arterial Structure as Well as the Gastrointestinal and Genitourinary Tracts. Analysis of *SMMHC-Cre^{ERT2}/Myocd$^{F/F}$* conditional mutant mice 4 mo following tamoxifen treatment revealed marked dilation and degeneration of the ascending aorta extending through the aortic arch compared with *Myocd$^{F/F}$* controls (Fig. 1*B*). Micro-computer tomographic (CT) imaging revealed dilation of the ascending aorta and aortic arch 4 mo following tamoxifen treatment of *SMMHC-Cre^{ERT2}/Myocd$^{F/F}$* mice compared with controls (Fig. S2 *A* and *B*). High-resolution echocardiographic analysis revealed that the mean diameter of the proximal aorta was 2.14 ± 0.12 mm in tamoxifen-treated *SMMHC-Cre^{ERT2}/Myocd$^{F/F}$* mice versus 1.74 ± 0.09 mm in control mice ($P < 0.05$) (Fig. S2 *C* and *D*). Histological examination

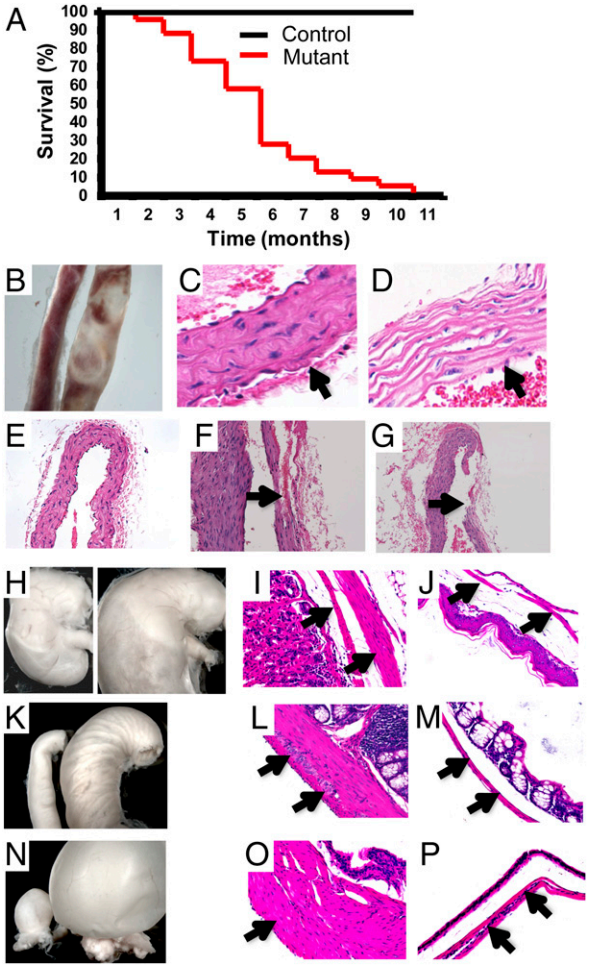

Fig. 1. *SMMHC-Cre^{ERT2}/Myocd$^{F/F}$* mutant mice succumb from defects in the vasculature and visceral tissues. (*A*) Kaplan–Meier survival curves for tamoxifen-treated control *Myocd$^{F/F}$* mice ($n = 60$) (black line) and *SMMHC-Cre^{ERT2}/Myocd$^{F/F}$* mice (red line) ($n = 60$). (*B*) Representative aorta harvested 4 mo following tamoxifen exposure of a *Myocd$^{F/F}$* control mouse (*Left*) and *SMMHC-Cre^{ERT2}/Myocd$^{F/F}$* mutant mouse (*Right*). (*C* and *D*) H&E-stained section cut at the level of the ascending aorta harvested 4 mo following tamoxifen treatment of a *Myocd$^{F/F}$* control mouse (*C*) and *SMMHC-Cre^{ERT2}/Myocd$^{F/F}$* mutant mouse (*D*). Arrows identify the aortic tunica media. Original magnification, 400×. (*E–G*) H&E-stained serial sections cut at the level of the ascending aorta in a tamoxifen-treated *Myocd$^{F/F}$* control (*E*, 200×) and *SMMHC-Cre^{ERT2}/Myocd$^{F/F}$* mutant (*F*, 400×; *G*, 200×) mouse demonstrating aortic dissections with disruption of the tunica intima generating a false lumen (arrow, *F*) and arterial rupture (arrow, *G*). (*H*) Stomach harvested 4 mo following tamoxifen exposure harvested from a *Myocd$^{F/F}$* control mouse (*Left*) and *SMMHC-Cre^{ERT2}/Myocd$^{F/F}$* mutant mouse (*Right*). (*I* and *J*) H&E-stained sections cut through the stomach of *Myocd$^{F/F}$* control mouse (*I*) and *SMMHC-Cre^{ERT2}/Myocd$^{F/F}$* mutant mouse (*J*) with arrows demarcating the muscularis mucosa. Original magnification, 200×. (*K*) Small intestine harvested 4 mo following tamoxifen exposure harvested from a *Myocd$^{F/F}$* control mouse (*Left*) and *SMMHC-Cre^{ERT2}/Myocd$^{F/F}$* mutant mouse (*Right*). (*L* and *M*) H&E-stained sections cut through the small intestine of *Myocd$^{F/F}$* control mouse (*L*) and *SMMHC-Cre^{ERT2}/Myocd$^{F/F}$* mutant mouse (*M*) with arrows demarcating the muscularis mucosa. (*N*) Bladder harvested 4 mo following tamoxifen exposure harvested from a *Myocd$^{F/F}$* control mouse (*Left*) and *SMMHC-Cre^{ERT2}/Myocd$^{F/F}$* mutant mouse (*Right*). (*O* and *P*) H&E-stained sections cut through the bladder of *Myocd$^{F/F}$* control mouse (*O*) and *SMMHC-Cre^{ERT2}/Myocd$^{F/F}$* mutant mouse (*P*) with arrows demarcating the muscularis mucosa. *L*, *M*, *O*, and *P*, original magnification, 400×.

of the aorta 4 mo following tamoxifen treatment of conditional mutant ($n = 10$) and *Myocd$^{F/F}$* control ($n = 10$) mice revealed medial (arrow) disarray with apparent SMC loss in the mutant

arteries (compare Fig. 1*C* with Fig. 1*D*). Loss of the characteristic spindle-like vascular SMC morphology was observed in all tamoxifen-treated conditional mutant arteries (Fig. 1*D*) compared with controls (Fig. 1*C*). Thrombosis, aneurysm, dissection with formation of false arterial lumen (arrow), and arterial rupture were variably observed in the aorta, carotid, and pulmonary arteries (compare Fig. 1*E* with Fig. 1 *F* and *G*).

In addition to changes in the vasculature, gross structural derangements were observed throughout the gastrointestinal and genitourinary tracts of tamoxifen-treated *SMMHC-Cre^{ERT2}/Myocd$^{F/F}$* mutant mice (Fig. 1 *H–P*). Four months following tamoxifen exposure, dilation of the stomach (Fig. 1*H*), small intestine (Fig. 1*K*), and bladder (Fig. 1*N*) was observed. Histologically, profound atrophy and disruption of the muscularis mucosa layer (arrows) developed in each of these visceral tissues (Fig. 1 *I*, *J*, *L*, *M*, *O*, and *P*). This was accompanied by the obvious loss of SMCs with separation within the muscularis mucosa of the stomach, intestine, and bladder of conditional *Myocd* mutant mice (Fig. 1 *J*, *M*, and *P*).

Myocardin Is Required for Maintenance of the Smooth Muscle Contractile Phenotype in Vascular and Visceral SMCs. As anticipated, robust expression of smooth muscle actin (SMA), smooth muscle myosin heavy chain (SMMHC), SM22α, calponin-h1, and myosin light chain kinase (MLCK) was observed in medial SMCs populating the aorta of tamoxifen-treated *Myocd$^{F/F}$* control mice (Fig. 2 *A–E*). By contrast, 4 mo following tamoxifen exposure, near absence of these SMC contractile proteins was observed in *SMMHC-Cre^{ERT2}/Myocd$^{F/F}$* SMCs populating the aorta (Fig. 2 *F–J*). qRT-PCR analyses confirmed that 4 mo following tamoxifen exposure, myocardin mRNA decreased by 85% in conditional mutant versus control mice (Fig. 2 *K* and *L*). Moreover, expression of the SMMHC, SM22α, SMA, caldesmon, and calponin genes decreased by 80–90% compared with aortas harvested from control mice (Fig. 2 *K* and *L*).

To examine whether expression of extracellular matrix (ECM) proteins compensated, at least in part, for the loss of SMC contractile proteins, we assessed fibrosis and expression of ECM in aortic sections harvested 4 mo following tamoxifen treatment of control (Fig. 2 *M–P*) and conditional mutant mice (Fig. 2 *Q–T*). Masson's trichrome staining revealed a marked reduction of SMC cytoplasm (red stain) accompanied by the robust induction of fibrosis (blue stain) in the tunica media of *SMMHC-Cre^{ERT2}/Myocd$^{F/F}$* mutant mice (Fig. 2*M*) compared with controls (Fig. 2*Q*). Of note, no difference in adventitial fibrosis was observed between control and mutant mice. Staining for tropoelastin (black stain) revealed no differences in expression in tamoxifen-treated control and conditional *Myocd$^{F/F}$* mutant mice with generalized preservation of lamellar organization (Fig. 2 *N* and *R*). However, a marked increase in fibronectin and laminin expression was observed in tamoxifen-treated *SMMHC-Cre^{ERT2}/Myocd$^{F/F}$* mice (Fig. 2 *O* and *P*) compared with *Myocd$^{F/F}$* controls (Fig. 2 *S* and *T*). Consistent with these observations, electron microscopy revealed the loss of contractile elements (Myo) accompanied by the expansion of the ER and ribosomes in medial SMCs following *Myocd* ablation (compare Fig. 2 *U* and *V* with Fig. 2 *W* and *X*). In addition, abundant fibrinous collagen (Col) was observed in tamoxifen-treated conditional mutant mice (Fig. 2*X*). Although it was difficult to appreciate due to the obvious loss of SMCs, expression of SMMHC and SMA appeared to be down-regulated in the muscularis mucosa layer of the stomach, small intestine, and bladder of tamoxifen-treated conditional mutant mice (Fig. S3). Taken together, these data reveal that during postnatal development, myocardin is required for maintenance of the contractile SMC phenotype and the loss of myocardin is accompanied by the induction of ECM proteins.

Loss of Myocardin Triggers Autophagy in Aortic SMCs. To examine whether the loss of myocardin activates a stress-induced autophagy program, aortic sections harvested from conditional mutant and control mice 14 d posttamoxifen exposure were immunostained for a panel of autophagy markers (Fig. 3 *A–J*) (9, 10). Elevated expression of Beclin-1 (green stain) was observed in the aorta of *SMMHC-Cre^{ERT2}/Myocd$^{F/F}$* conditional mutant mice (Fig. 3*F*) but not *Myocd$^{F/F}$* controls (Fig. 3*A*). Similarly, autophagy-related

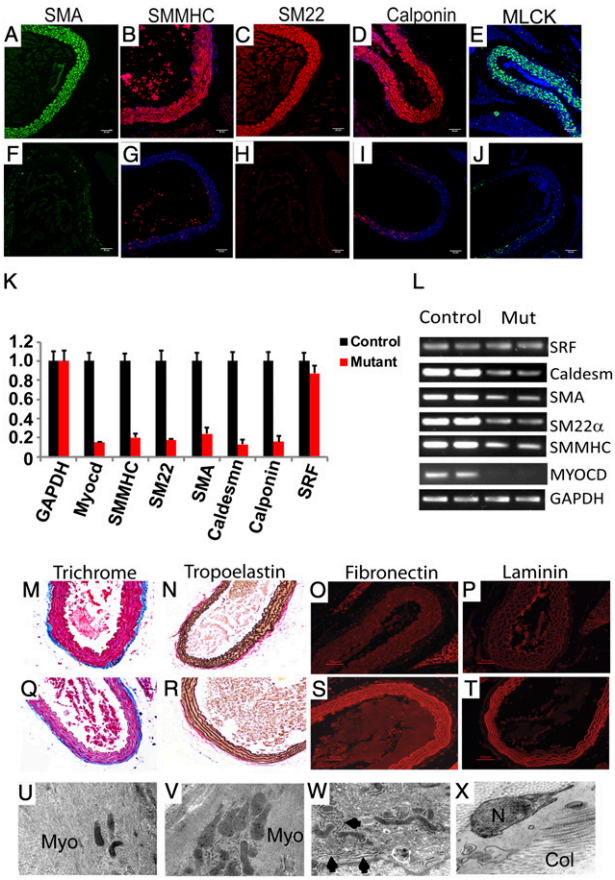

Fig. 2. Myocardin-deficient aortic SMCs exhibit markedly diminished expression of SMC contractile proteins and induction of ECM. (*A–J*) Four months following tamoxifen treatment, aortic sections prepared from *Myocd$^{F/F}$* control mice (*A–E*) demonstrate robust expression of SMA (green), SMMHC (red), SM22α (red), calponin-h1 (red), and MLCK (green). By contrast, SMC contractile proteins are barely detectable in aortic sections prepared from tamoxifen-treated *SMMHC-Cre^{ERT2}/Myocd$^{F/F}$* mutant mice (*F–J*). (*K*) qRT-PCR demonstrating 80–90% decrease in expression of genes encoding myocardin (Myocd), SMMHC, SM22α, SMA, caldesmon, and calponin-h1 in tamoxifen-treated *SMMHC-Cre^{ERT2}/Myocd$^{F/F}$* mutant mice (red bars) compared with *Myocd$^{F/F}$* control mice (black bars). Data are expressed as mean gene expression (arbitrary units) ± SEM. (*L*) Representative ethidium bromide-stained agarose gel showing relative levels of gene expression of myocardin, SRF, and SMC contractile genes (SMA, SMMHC, SM22α, Caldesmon) in qRT-PCR amplified mRNA harvested from tamoxifen-treated *Myocd$^{F/F}$* (Control) and *SMMHC-Cre^{ERT2}/Myocd$^{F/F}$* mutant (Mut) mice. (*M–T*) Aortic sections harvested from tamoxifen-treated *Myocd$^{F/F}$* control (*M–P*) and *SMMHC-Cre^{ERT2}/Myocd$^{F/F}$* mutant (*Q–T*) mice were stained with Masson's trichrome (*M* and *Q*) or immunostained with antibodies that detect tropoelastin (*N* and *R*), fibronectin (*O* and *S*), or laminen (*P* and *T*). Masson's trichrome staining reveals loss of SMC cytoplasm (red stain) and induction of medial fibrosis (blue stain) in the *Myocd* mutant aorta (*Q*) compared with the control (*M*). Tropoelastin immunostaining (black) reveals preservation of lamellar architecture (*N* and *R*). However, a dramatic induction of fibronectin (red) and laminin (red) are observed in the aorta of tamoxifen-treated *Myocd* mutant mice (*S* and *T*) compared with controls (*O* and *P*). (*U–V*) Electron micrographs of sections prepared from the ascending aorta harvested 4 mo following tamoxifen treatment of *Myocd$^{F/F}$* mice (*U* and *V*) and *SMMHC-Cre^{ERT2}/Myocd$^{F/F}$* mutant mice (*W* and X). Abundant myofibers (Myo) are observed throughout the cytoplasm of the control mouse (*U* and *V*). By contrast, contractile fibers are not observed in the cytoplasm of vascular SMCs of *SMMHC-Cre^{ERT2}/Myocd$^{F/F}$* mutant mice (*W* and *X*). However, abundant fibrinous collagen (Col) is observed in the extracellular spaces (*W* and *X*). *U*, *V*, *W*, and *X*, original magnification, 50,000×.

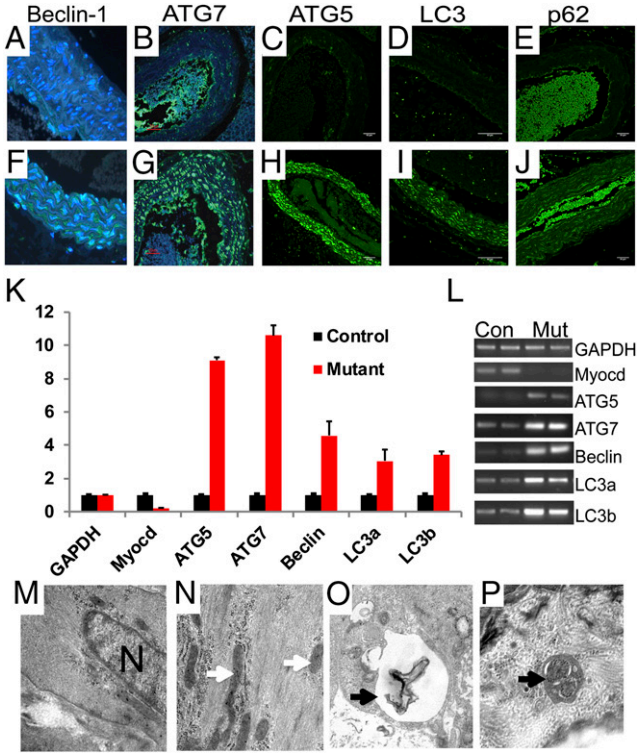

Fig. 3. *Myocd* deletion triggers autophagy in SMCs populating the aorta. (*A–J*) Immunohistochemical analysis performed on aortic sections harvested 14 d following tamoxifen treatment of $Myocd^{F/F}$ control (*A–E*) and *SMMHC-*Cre^{ERT2}*/*$Myocd^{F/F}$ mutant mice (*F–J*) reveals marked induction of Beclin-1 (green), ATG7 (green), ATG5 (green), LC3 (green), and p62 (green) in medical SMCs of *SMMHC-*Cre^{ERT2}*/*$Myocd^{F/F}$ mutant mice. Original magnification, 400× (*A* and *F*) and 200× (*B–E* and *G–J*). (*K*) qRT-PCR demonstrating 3–10-fold induction of genes encoding ATG5, ATG7, Beclin-1, LC3a, and LC3b in tamoxifen-treated *SMMHC-*Cre^{ERT2}*/*$Myocd^{F/F}$ mutant mice (red bars) compared with $Myocd^{F/F}$ control mice (black bars). Data are expressed as mean gene expression (arbitrary units) ± SEM. (*L*) Representative ethidium bromide-stained agarose gel showing relative levels of autophagy-related gene expression in qRT-PCR amplified mRNA harvested from tamoxifen-treated $Myocd^{F/F}$ (Con) and *SMMHC-*Cre^{ERT2}*/*$Myocd^{F/F}$ mutant (Mut) mice. (*M–P*) Electron micrographs of aortic SMCs harvested 14 d following tamoxifen treatment of *SMMHC-*Cre^{ERT2}*/*$Myocd^{F/F}$ mutant mice. As anticipated, abundant myofibers and mitochondria (arrows) in $Myocd^{F/F}$ control vascular SMCs (*M* and *N*). By contrast, evidence of cellular stress (vacuoles) and autophagosomes (arrows) was observed in the cytoplasm of SMCs populating the aorta of *SMMHC-*Cre^{ERT2}*/*$Myocd^{F/F}$ mutant mice (*O* and *P*). Original magnification, 50,000×.

protein 7 (ATG7) (green stain) and ATG5 (green stain) were observed in arteries of *SMMHC-*Cre^{ERT2}*/*$Myocd^{F/F}$ mutant mice (Fig. 3 *G* and *H*), but not in control mice (compare Fig. 3*B* with Fig. 3*C*). Moreover, microtubule-associated protein 1 light chain 3 (LC3) and p62, or sequestosome 1, were dramatically up-regulated in arteries of conditional mutant mice (green stain, compare Fig. 3 *D* and *E* with Fig. 3 *I* and *J*). qRT-PCR revealed 3–10-fold induction of ATG5, ATG7, Beclin-1, LC3a, and LC3b gene expression in the aorta of tamoxifen-treated *SMMHC-*Cre^{ERT2}*/*$Myocd^{F/F}$ mice ($n = 3$) compared with the expression of these genes in $Myocd^{F/F}$ control mice ($n = 3$) ($P < 0.05$) (Fig. 3 *K* and *L*). Fourteen days following tamoxifen treatment, electron microscopy revealed abundant myofibers and mitochondria (white arrows) in medial SMCs populating the aorta of $Myocd^{F/F}$ control mice (Fig. 3 *M* and *N*). By contrast, a generalized loss of myofibers accompanied by formation of electron-dense structures resembling autophagosomes with embedded membranes and organelles (arrows) were observed in SMCs populating the aorta of *SMMHC-*Cre^{ERT2}*/*$Myocd^{F/F}$ mutant mice (Fig. 3 *O* and *P*).

Loss of Myocardin Induces Cell Autonomous Autophagy. To distinguish whether SMC autophagy results from the cell autonomous loss of myocardin versus hemodynamic or other systemic stress, primary cultures of mouse aortic SMCs harvested from $Myocd^{F/F}$ conditional mutant mice were infected with a replication-defective adenovirus encoding Cre (Ad-Cre) or the control virus Ad-LacZ encoding β-galactosidase. Western blot analysis confirmed that myocardin protein decreased by 90% in SMC cultures infected with Ad-Cre relative to levels of myocardin expression observed in Ad-LacZ–infected cells (Fig. 4*G*). Remarkably, 48 h postinfection in cells expressing Cre recombinase (red stain, Fig. 4 *A–C*), dramatic induction of ATG5, ATG7, and LC3 (green stain) was observed (Fig. 4 *D–F*). Consistent with these data, immunoblot analysis revealed robust induction of Beclin-1, ATG5, ATG7, and LC3 in Ad-Cre–transduced $Myocd^{F/F}$ vascular SMCs (Fig. 4*G*).

***Myocd* Deletion Activates ER Stress and Unfolded Protein Response in Isolated Aortic SMCs.** Electron microscopy of tamoxifen-treated *SMMHC-*Cre^{ERT2}*/*$Myocd^{F/F}$ aortic SMCs revealed dilation of the ER (Fig. S4), suggesting the activation of the ER stress pathway (for review, see refs. 11, 12). To examine the hypothesis that the ER stress pathway or unfolded protein response (UPR) is activated in response to the loss of myocardin, we surveyed the expression of mediators of ER stress in Ad-Cre– and control Ad-LacZ–transduced $Myocd^{F/F}$ primary aortic SMCs. At 48 h postinfection, a dramatic induction of phosphorylated PERK was observed in Ad-Cre– but not Ad-LacZ–transduced SMCs (Fig. 4 *H* and *M*). Consistent with this observation, phosphorylated cytoplasmic eIF-2a (green stain), which is phosphorylated by PERK coupling ER stress to accumulation of protein, was observed in Ad-Cre–transduced SMCs (Fig. 4 *I* and *N*). As anticipated, in response to phosho–eIF-2a, ATF4 (green stain) was up-regulated in the nucleus of Ad-Cre– but not Ad-LacZ–transduced SMCs (Fig. 4 *J* and *O*). Moreover, CHOP (green stain), which is induced in response to ER stress and promotes apoptosis, was

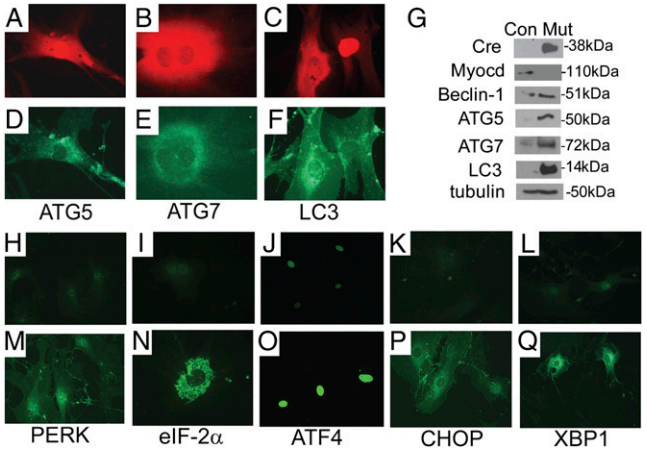

Fig. 4. *Myocd* ablation triggers SMC autonomous autophagy and ER stress. (*A–G*) *Myocd* gene ablation triggers autophagy in primary cultures of aortic SMCs. $Myocd^{F/F}$ SMCs were transduced with Ad-Cre or Ad-LacZ (control). At 48 h posttransduction, SMCs were fixed and immunostained with antibodies that recognize Cre recombinase or ATG5, ATG7, or LC3. In cells undergoing Cre-mediated *Myocd* gene deletion (red stain, *A–C*), robust expression of ATG5, ATG7, and LC3 is observed (green stain, *D–F*). Original magnification, 400×. (*G*) Western blot analysis of protein lysates harvested from Ad-LacZ– (Con) or Ad-Cre– (Mut) transduced SMCs incubated with antibodies that recognize Cre, myocardin (Myocd), Beclin-1, ATG-5, ATG-7, LC3, and tubulin (control). Molecular weight markers are shown to the right of the blot. (*H–Q*) $Myocd^{F/F}$ SMCs were transduced with Ad-LacZ (*H–L*) or Ad-Cre (*M–Q*). At 48 h posttransduction, SMCs were fixed and immunostained with antibodies that recognize Cre recombinase or PERK, eIF-2a, ATF4, CHOP, or XBP1. In Ad-Cre–transduced cells, robust expression (green stain) of PERK, eIF-2a, nuclear ATF4, CHOP, and XBP-1 is observed.

observed in Ad-Cre– but not Ad-LacZ–transduced SMCs (Fig. 4 *K* and *P*). In addition, nuclear-spliced XBP-1 (green stain) was also observed in Ad-Cre– but not in Ad-LacZ–transduced SMCs (Fig. 4 *L* and *Q*). Finally, it is noteworthy that comparable levels of mTOR and AMP kinase expression, which operate both upstream and downstream of ER stress signals (13), were observed in Ad-Cre– and Ad-LacZ–transduced $Myocd^{F/F}$ SMCs.

Late-Stage Induction of Apoptosis in Vascular SMCs. Autophagy may serve to preserve energy homeostasis within the cell, but under certain conditions, cell stress may induce programmed cell death (9, 10). To examine this question, we surveyed expression of apoptotic markers 14 d and 4 mo following tamoxifen exposure. Surprisingly, 14 d following tamoxifen exposure, nuclear TUNEL staining (green) indicative of apoptosis was not observed in medial SMCs populating the aorta of $SMMHC\text{-}Cre^{ERT2}/Myocd^{F/F}$ mutant or control mice (Fig. 5 *A* and *F*). By contrast, 4 mo following tamoxifen exposure, a dramatic induction of TUNEL-positive SMCs populating the aorta was observed in $SMMHC\text{-}Cre^{ERT2}/Myocd^{F/F}$ mutant mice compared with $Myocd^{F/F}$ control mice (Fig. 5 *B* and *G*). The apoptotic index (percentage medial SMCs with TUNEL-positive nuclei) was 22.1 ± 0.01% in mutant mice compared with 3.99 ± 0.01% in controls ($P < 0.01$). Interestingly, focal patches of TUNEL-positive cells were often observed following tamoxifen treatment of $SMMHC\text{-}Cre^{ERT2}/Myocd^{F/F}$ mutant mice (Fig. S5 *B–D* and *F–H*) but not in controls (Fig. S5 *A* and *E*). Consistent with these findings, 4 mo following tamoxifen exposure, abundant caspase 3 and caspase 9 (arrows) were observed in SMCs of tamoxifen-treated $SMMHC\text{-}Cre^{ERT2}/Myocd^{F/F}$ mutant mice, demonstrating activation of the intrinsic/mitochondrial apoptotic pathway (Fig. 5 *C*, *D*, *H*, and *I*). Moreover, p53, a major orchestrator of cellular response to stress, was induced in medial SMCs of tamoxifen-treated conditional mutant mice (Fig. 5 *E* and *J*). Consistent with these observations, 4 mo following tamoxifen treatment, EM revealed widespread SMC apoptosis manifest as nuclear (N) chromatin aggregation (arrows), nuclear fragmentation, and cytoplasmic apoptotic body (AB) formation in tamoxifen-treated $SMMHC\text{-}Cre^{ERT2}/Myocd^{F/F}$ mutant mice (Fig. 5 *M* and *N*). By contrast, preserved nuclear architecture with diffuse chromatin and abundant myofibers was observed in SMCs populating the aorta of tamoxifen-treated $Myocd^{F/F}$ control mice (Fig. 5 *K* and *L*).

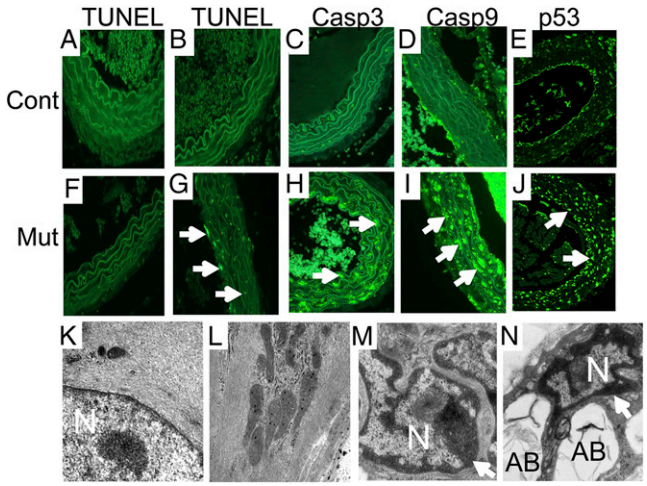

Fig. 5. Late-stage induction of apoptosis in myocardin-deficient aortic SMCs. At 14 d (*A* and *F*) and 4 mo (*B–E* and *G–J*) following tamoxifen treatment, the aorta isolated from $Myocd^{F/F}$ (Cont) and $SMMHC\text{-}Cre^{ERT2}/Myocd^{F/F}$ (Mut) mice were fixed, sectioned, and TUNEL-stained or immunostained to survey apoptosis. (*A*, *B*, *F*, and *G*) Representative photomicrographs demonstrate only rare TUNEL-positive nuclei (green) in the control (*A*) or conditional mutant (*F*) aorta 14 d following tamoxifen treatment. By contrast, 4 mo following tamoxifen exposure, widespread TUNEL-positive nuclei (arrows) are observed in the $SMMHC\text{-}Cre^{ERT2}/Myocd^{F/F}$ mutant aorta (*G*) but not in the control (*B*). In addition, activated caspase 3 (arrow, green stain), caspase 9 (arrow, green stain), and p53 (arrows) are observed in medial SMCs populating the aorta of tamoxifen-treated $SMMHC\text{-}Cre^{ERT2}/Myocd^{F/F}$ mutant mice (*H–J*) but not in control mice (*C–E*). Original magnification, 400×. (*K–N*) EM of aortic sections prepared from tamoxifen-treated $Myocd^{F/F}$ control (*K* and *L*) and $SMMHC\text{-}Cre^{ERT2}/Myocd^{F/F}$ mutant (*M* and *N*) mice reveals preserved nuclear (N) architecture with dispersed chromatin and abundant myofibers in vascular SMCs (*K* and *L*). By contrast, nuclear chromatin condensation (arrows), nuclear fragmentation, and cytoplasmic apoptotic body (AB) formation are observed in SMCs populating the aorta of $SMMHC\text{-}Cre^{ERT2}/Myocd^{F/F}$ mutant mice (*M* and *N*). Original magnification, 50,000×.

Discussion

The data described in this report demonstrate a unique, and important, function of the muscle-restricted transcriptional coactivator, myocardin, during postnatal development in the vasculature and visceral tissues. In the aorta and other arteries, *Myocd* deletion leads to disruption of the tunica media, dilation of the thoracic aorta, aneurysm, and dissection. In the gastrointestinal and genitourinary tract, disruption and atrophy of the muscularis mucosa is observed leading to dilation of the stomach, intestine, bladder, and ureters. In both vascular and visceral SMCs, the loss of myocardin causes a profound block in the expression of SMC contractile genes and proteins. This is surprising, as Srf, Mkl-1, and Mkl-2 are expressed and induced in tamoxifen-treated *Myocd* conditional mutant mice, suggesting strongly that myocardin is the sole MRTF member capable of activating the repertoire of SRF-dependent SMC genes during postnatal development. Moreover, we believe that this is the first direct evidence that myocardin regulates the contractile phenotype in visceral SMCs populating the gastrointestinal and urinary tracts.

Remarkably, hours to days following ablation of *Myocd*, SMCs activate an autophagic program manifested by expression of Beclin-1, ATG5, ATG7, and LC3. Early and late autophagosomes containing organelles were observed in vascular SMCs (Fig. 3). Of note, autophagy was not only observed in the vasculature of *Myocd* conditional mutant mice but also in *Myocd*-deficient isolated vascular SMCs (Fig. 4). The observation that multiple markers of ER stress/UPR were induced following the ablation of *Myocd* in aortic SMCs suggests strongly that ER stress/UPR may contribute to the activation of the autophagic program. Activation of autophagy occurred coincident with the loss of myocardin, raising the intriguing hypothesis that modulation of the vascular SMC phenotype (and repression of SMC contractile genes) may be accelerated by ER stress-induced autophagy of SMC contractile elements required to preserve cellular energy stores and metabolism. Consistent with a model wherein turnover of SMC contractile proteins triggers ER stress-induced autophagy, overexpression of SMMHC led to the activation of UPR and autophagic turnover in vascular SMCs (14). However, late-stage SMC apoptosis was observed, suggesting that induction of autophagy is ultimately not sufficient to preserve vascular (and visceral) SMCs required for cardiovascular homeostasis and function of visceral tissues.

Remarkably, within weeks of *Myocd* deletion, all tamoxifen-treated $SMMHC\text{-}Cre^{ERT2}/Myocd^{F/F}$ mutant mice developed dilation of the ascending aorta and aortic arch, recapitulating pathologies observed in TAAD patients. As such, these findings provide insights into the pathogenesis of heritable causes of TAAD (8). Ten to fifteen percent of TAAD patients exhibit a heterozygous mutation in the myocardin target gene *ACTA2* or *MYH11* (15, 16). *MYH11* mutations are identified primarily in families with TAAD inherited in association with a PDA (17). Consistent with this observation, mice harboring a neural crest-restricted deletion of *Myocd* succumb within the perinatal period from hypoxia attributable to PDA (17). Taken together, these data implicate the loss of myocardin-activated SMC contractile genes in development of thoracic aortic dissection and aneurysms observed in *Myocd* conditional mutant mice. The association of focal patches of apoptosis in the aorta of tamoxifen-treated $SMMHC\text{-}Cre^{ERT2}/Myocd^{F/F}$ conditional

mutant mice raises the intriguing hypothesis that mutations in the *ACTA2* and/or *MYH11* genes may initially only lead to dilation of the thoracic aorta, but over time in response to hemodynamic or prolonged ER stress result in medial SMC apoptosis, leading to aortic dissection and its associated morbidities.

The accompanying disruption of the muscularis mucosa throughout the gastrointestinal and genitourinary tracts provides, to our knowledge, the first direct evidence that myocardin lies upstream in a transcriptional program required for maintenance of the SMC contractile phenotype in visceral SMCs. We speculate that as in vascular SMCs, the gross alterations in visceral tissues are, at least in part, attributable to the loss of SRF/myocardin-activated SMC contractile genes. In support of this model, *MYH11*-deficient mice demonstrated vascular complications as well as dysfunction of bladder and intestine (18, 19). Moreover, de novo mutations in *ACTA2* causes multisystem smooth muscle dysfunction that includes aortic and cerebrovascular disease, fixed dilated pupils, hypotonic bladder, malrotation, and hypoperistalsis of the gut (20). Taken together, these observations suggest that further study of mutations in genes encoding SMC contractile proteins may provide new insights into gastrointestinal and genitourinary syndromes, including esophageal reflux, gastrointestinal dysmotility syndromes, irritable bowel syndromes, and bladder dysmotility.

Methods

Generation of Mice Containing a SMC-Restricted Mutation in the *Myocd* Gene. Genetically engineered mice harboring a conditional null mutation in the *Myocd* gene ($Myocd^{F/F}$) were described previously (6, 7). $SMMHC\text{-}Cre^{ERT2}$ mice, which express tamoxifen-inducible Cre recombinase under the transcriptional control of the *SMMHC* (*Myh11*) promoter, were provided by Stefan Offermanns, Max Planck Institute, Bad Nauheim, Germany (21). To ablate the *Myocd* gene in SMCs, 2-mo-old $SMMHC\text{-}Cre^{ERT2}/Myocd^{F/F}$ conditional mutant mice or $Myocd^{F/F}$ controls received 65 mg/kg i.p. injection of tamoxifen daily for 4 d. Mice were euthanized 10 d, 14 d, 21 d, or 4 mo following initiation of tamoxifen treatment. All animal experimentation was performed under protocols approved by the University of Pennsylvania Institutional Animal Care and Use Committee and in accordance with National Institutes of Health guidelines.

Echocardiography and Micro-CT Imaging. Transthoracic echocardiography was performed as described previously (6). Analyses of left ventricular mass and volume, ejection fraction (EF %), and fraction shortening (FS %) were performed using standard 2D quantification methods by following the guidelines of the America Society of Echocardiography (22). Micro-CT imaging was performed on an eXplore Locus SP specimen scanner as described (GE Healthcare) (21). Scan protocol included 80 keV, 80 μA, 250-μm Al filter, short-scan (Parker) method, 500 views at 0.4° steps, four averages, $8 \times 8 \times 8$ μm^3 reconstruction voxel, and 3.5-h scan time. Image data were analyzed with MicroView (GE Healthcare), ImageJ (National Institutes of Health), and OsiriX software.

Histology, Immunohistochemistry, and Electron Microscopy. Histology, immunohistochemistry, and electron microscopy were performed as described previously (7). Immunohistochemistry protocols are available at www.pennmedicine.org/heart/research-clinical-trials/core-facilities/histology-gene-expression/. Antibodies used for immunohistochemistry studies are included in Table S1.

Real-Time qRT-PCR and Western Blot Analysis. qRT-PCR was performed using the DNA Engine Opticon 2 Real Time Detection System (Bio-Rad Laboratories, Inc.) as described previously (23). Western blot analyses were performed and quantified as described previously (7). Antibodies are described in Table S1.

RdAV Transduction of SMCs and Quantification of Autophagy. Primary cultures of mouse aortic SMCs were isolated from 1-mo-old $Myocd^{F/F}$ conditional mutant mice as described previously (24). Early (<4) passage vascular SMCs were used in the autophagy and ER stress experiments. Triplicate cultures of vascular SMCs were grown in low serum medium (DMEM containing 0.5% FBS and 0.3% horse serum) for 24 h and infected with (10 multiplicity of infection) Ad-LacZ or Ad-Cre as described previously (24). At 48 h post-transduction, triplicate cultures were harvested for protein assays or immunostaining as described previously (7, 24). Experiments were repeated three times to ensure reproducibility.

Statistical Considerations. Comparison of survival rates was performed by Kaplan–Meier analysis with PRISM software (GraphPad). All measurement data are expressed as mean ± SEM. The statistical significance of differences between groups was determined by Student's *t* test. Differences were considered significant at a P value < 0.05.

ACKNOWLEDGMENTS. This work was supported in part by National Institutes of Health Grants R01-HL094520 and R01-HL102969.

1. Owens GK, Kumar MS, Wamhoff BR (2004) Molecular regulation of vascular smooth muscle cell differentiation in development and disease. *Physiol Rev* 84(3):767–801.
2. Parmacek MS (2007) Myocardin-related transcription factors: Critical coactivators regulating cardiovascular development and adaptation. *Circ Res* 100(5):633–644.
3. Pipes GC, Creemers EE, Olson EN (2006) The myocardin family of transcriptional coactivators: Versatile regulators of cell growth, migration, and myogenesis. *Genes Dev* 20(12):1545–1556.
4. Wang DZ, et al. (2002) Potentiation of serum response factor activity by a family of myocardin-related transcription factors. *Proc Natl Acad Sci USA* 99(23):14855–14860.
5. Huang J, et al. (2012) Myocardin regulates BMP10 expression and is required for heart development. *J Clin Invest* 122(10):3678–3691.
6. Huang J, et al. (2009) Myocardin is required for cardiomyocyte survival and maintenance of heart function. *Proc Natl Acad Sci USA* 106(44):18734–18739.
7. Huang J, et al. (2008) Myocardin regulates expression of contractile genes in smooth muscle cells and is required for closure of the ductus arteriosus in mice. *J Clin Invest* 118(2):515–525.
8. Milewicz DM, et al. (2008) Genetic basis of thoracic aortic aneurysms and dissections: Focus on smooth muscle cell contractile dysfunction. *Annu Rev Genomics Hum Genet* 9:283–302.
9. Green DR, Levine B (2014) To be or not to be? How selective autophagy and cell death govern cell fate. *Cell* 157(1):65–75.
10. Choi AM, Ryter SW, Levine B (2013) Autophagy in human health and disease. *N Engl J Med* 368(19):1845–1846.
11. Bravo R, et al. (2013) Endoplasmic reticulum and the unfolded protein response: Dynamics and metabolic integration. *Int Rev Cell Mol Biol* 301:215–290.
12. Dufey E, Sepúlveda D, Rojas-Rivera D, Hetz C (2014) Cellular mechanisms of endoplasmic reticulum stress signaling in health and disease. 1. An overview. *Am J Physiol Cell Physiol* 307(7):C582–C594.
13. Appenzeller-Herzog C, Hall MN (2012) Bidirectional crosstalk between endoplasmic reticulum stress and mTOR signaling. *Trends Cell Biol* 22(5):274–282.
14. Kwartler CS, et al. (2014) Overexpression of smooth muscle myosin heavy chain leads to activation of the unfolded protein response and autophagic turnover of thick filament-associated proteins in vascular smooth muscle cells. *J Biol Chem* 289(20):14075–14088.
15. Guo DC, et al. (2007) Mutations in smooth muscle alpha-actin (ACTA2) lead to thoracic aortic aneurysms and dissections. *Nat Genet* 39(12):1488–1493.
16. Kuang SQ, et al. (2012) Rare, nonsynonymous variant in the smooth muscle-specific isoform of myosin heavy chain, MYH11, R247C, alters force generation in the aorta and phenotype of smooth muscle cells. *Circ Res* 110(11):1411–1422.
17. Zhu L, et al. (2006) Mutations in myosin heavy chain 11 cause a syndrome associating thoracic aortic aneurysm/aortic dissection and patent ductus arteriosus. *Nat Genet* 38(3):343–349.
18. Babu GJ, et al. (2001) Loss of SM-B myosin affects muscle shortening velocity and maximal force development. *Nat Cell Biol* 3(11):1025–1029.
19. Morano I, et al. (2000) Smooth-muscle contraction without smooth-muscle myosin. *Nat Cell Biol* 2(6):371–375.
20. Milewicz DM, et al. (2010) De novo ACTA2 mutation causes a novel syndrome of multisystemic smooth muscle dysfunction. *Am J Med Genet A* 152A(10):2437–2443.
21. Wirth A, et al. (2008) G12-G13-LARG-mediated signaling in vascular smooth muscle is required for salt-induced hypertension. *Nat Med* 14(1):64–68.
22. Youn HJ, et al. (1999) Two-dimensional echocardiography with a 15-MHz transducer is a promising alternative for in vivo measurement of left ventricular mass in mice. *J Am Soc Echocardiogr* 12(1):70–75.
23. Du KL, et al. (2004) Megakaryoblastic leukemia factor-1 transduces cytoskeletal signals and induces smooth muscle cell differentiation from undifferentiated embryonic stem cells. *J Biol Chem* 279(17):17578–17586.
24. Lepore JJ, Cappola TP, Mericko PA, Morrisey EE, Parmacek MS (2005) GATA-6 regulates genes promoting synthetic functions in vascular smooth muscle cells. *Arterioscler Thromb Vasc Biol* 25(2):309–314.